JACS
JOURNAL OF THE AMERICAN CHEMICAL SOCIETY
pubs.acs.org/JACS
Communication

Probing Molecular Motions in Metal–Organic Frameworks by Three-Dimensional Electron Diffraction

Laura Samperisi, Aleksander Jaworski, Gurpreet Kaur, Karl Petter Lillerud, Xiaodong Zou,* and Zhehao Huang*

Cite This: J. Am. Chem. Soc. 2021, 143, 17947–17952
Read Online
ACCESS | Metrics & More | Article Recommendations | Supporting Information

ABSTRACT: Flexible metal–organic frameworks (MOFs) are known for their vast functional diversities and variable pore architectures. Dynamic motions or perturbations are among the highly desired flexibilities, which are key to guest diffusion processes. Therefore, probing such motions, especially at an atomic level, is crucial for revealing the unique properties and identifying the applications of MOFs. Nuclear magnetic resonance (NMR) and single-crystal X-ray diffraction (SCXRD) are the most important techniques to characterize molecular motions but require pure samples or large single crystals (>5 × 5 × 5 μm^3), which are often inaccessible for MOF synthesis. Recent developments of three-dimensional electron diffraction (3D ED) have pushed the limits of single-crystal structural analysis. Accurate atomic information can be obtained by 3D ED from nanometer- and submicrometer-sized crystals and samples containing multiple phases. Here, we report the study of molecular motions by using the 3D ED method in MIL-140C and UiO-67, which are obtained as nanosized crystals coexisting in a mixture. In addition to an *ab initio* determination of their framework structures, we discovered that motions of the linker molecules could be revealed by observing the thermal ellipsoid models and analyzing the atomic anisotropic displacement parameters (ADPs) at room temperature (298 K) and cryogenic temperature (98 K). Interestingly, despite the same type of linker molecule occupying two symmetry-independent positions in MIL-140C, we observed significantly larger motions for the isolated linkers in comparison to those reinforced by π–π stacking. With an accuracy comparable to that of SCXRD, we show for the first time that 3D ED can be a powerful tool to investigate dynamics at an atomic level, which is particularly beneficial for nanocrystalline materials and/or phase mixtures.

Structural flexibility is a unique characteristic of metal–organic frameworks (MOFs)/porous coordination polymers (PCPs).[1−6] It plays a central role in the host–guest chemistry and is attractive for a wide range of applications, including gas storage,[7−10] catalysis,[11−13] and separation.[14−17] In addition to the well-known phenomenon of breathing and swelling, local flexibilities, such as linker rotation and swing, are not accompanied by phase transitions yet play an important role in controlling the pore accessibility and diffusion rates of the guest molecules in the framework.[18−21] As the dynamic properties are closely associated with structural features, a deep understanding of MOFs, down to an atomic level, is essential for further development of rational design strategies and exploitation of their applications.

In MOF synthesis, it is often found that the same starting regents (i.e., metals and organic ligands) can lead to MOFs with different topologies, which are dictated by experimental thermodynamic and/or kinetic conditions.[22,23] The coexistence of different MOFs in the same sample hampers characterization by many techniques, such as nuclear magnetic resonance (NMR) and powder X-ray diffraction (PXRD), to unambiguously determine the structure–property relationship. Additionally, MOFs are often only obtained as nanosized crystals, which are too small to be studied by single-crystal X-ray diffraction (SCXRD). Transmission electron microscopy (TEM) provides unique advantages in investigating MOFs at an atomic level, even when they appear as a phase mixture. With the recent development of real-space TEM imaging techniques, direct observation of MOFs has been achieved at atomic resolution, which revealed changes during MOF formation, phase transition, and host–guest interactions.[24,25] While TEM imaging is advantageous for analyzing local structures, it can only be applied to limited MOFs that can stand relatively high electron doses. In comparison to imaging, three-dimensional electron diffraction (3D ED) requires a 2 magnitudes lower electron dose,[24] with a dose rate of approximately 0.01 $e^- A^{-2} s^{-1}$. The strong interaction between electrons and matter allows single-crystal 3D ED studies on nanometer-sized MOFs.[26−34] 3D ED thus offers an immerse opportunity to determine and refine 3D structures of beam-sensitive nanomaterials.[35−38]

Linker motions in MOFs (e.g., π-flips and small-angle librations) are commonly detected by solid-state NMR,[39,40] vibrational spectroscopy,[41] and inelastic neutron scattering.[42] Whereas SCXRD has also been used to elucidate dynamics in crystalline solids,[43−45] such studies have not been demonstrated by electron diffraction. Here, we present the first study of molecular motions in MOFs by 3D ED using the data

Received: August 9, 2021
Published: October 25, 2021

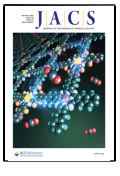

https://doi.org/10.1021/jacs.1c08354
J. Am. Chem. Soc. 2021, 143, 17947−17952

collection protocol of continuous rotation electron diffraction (cRED) developed in our group.[46] Using Zr as the metal source and 4,4′-biphenyldicarboxylate (bpdc) as the organic linker, UiO-67 and MIL-140C were synthesized in a phase mixture, with a $ZrCl_4$:H_2bpdc:benzoic acid:*N*,*N*-dimethylformamide (DMF):water molar ratio of 1:1:3:50:3 (Figures S1 and S2; see the Supporting Information for more details). This condition has been reported to synthesize UiO-67 with little missing-linker defects.[47] This phase mixture was used for the current study, and 3D ED has the unique advantage of studying multiphasic samples.[33,48]

The cRED data collected from the sample gave two distinct unit cells and space groups: one with the cubic space group $Fm\bar{3}m$ and a = 26.880(3) Å corresponding to UiO-67[49] (Figure S3) and the other with the monoclinic space group $C2/c$ and a = 32.360(7) Å, b = 15.800(3) Å, c = 7.910(2) Å, and β = 103.00(3)°, attributed to MIL-140C[50] (Figure S4). Details of data collection and space group determination are given in the Supporting Information. The structures of both MOFs were solved *ab initio* from cRED data using a single data set for UiO-67 and a merged data set from three different crystals for MIL-140C. All non-hydrogen atoms were found directly from the structure solution and refined with anisotropic atomic displacement parameters. The refinements converged to a R1 value of 0.215 for 404 observed reflections for UiO-67 and 0.169 for 2083 observed reflections for MIL-140C (Table S1).

UiO-67 is built by one 12-connected $Zr_6O_4(OH)_4$ cluster and one bpdc linker in the asymmetric unit, and its structure was previously determined by SCXRD.[51] The structural model refined against the cRED data shows severe elongations of the nonaxial carbon atoms of the bpdc linker (C3 and C4) in the thermal ellipsoid model (Figure 1a). As thermal ellipsoids represent the probability of atomic positions,[52] the elongations could be attributed to molecular motions of the bpdc linker. This observation is in good agreement with that simulated by molecular dynamics (Figure S5)[53] and obtained by SCXRD. Despite the fact that the cRED data have a much lower resolution (0.90 Å) in comparison to the SCXRD data (0.70 Å), the ellipsoids from cRED data have a comparable spatial coverage with the split atoms of the SCXRD model (Figure 1b).

In addition to the molecular motions, we also found an unusual elliptical behavior of the μ_3-O atom caused by the disorder in the Zr_6 cluster, which was also observed by SCXRD.[51] For the other atoms in the structure, the atomic positions of UiO-67 obtained by cRED and SCXRD exhibited an excellent agreement, with an average deviation of 0.018(1) Å (Table S2).

The structure of MIL-140C was previously reported by model building through reticular chemistry,[50] and its single-crystal analysis has not been achieved until this work. MIL-140C is built by Zr-oxo chains rather than Zr-oxo clusters. There are two bpdc linkers in the asymmetric unit. The Zr-oxo chains are aligned in parallel to [001] and are connected by linker 1 along the [110] and [1−10] directions and by linker 2 along [010]. The thermal ellipsoid model obtained from cRED data shows strong elongations of the nonaxial carbon atoms in linker 1 (Figure 2a). In contrast, the elongations are much smaller for the atoms in linker 2. The electrostatic potential map further confirms the difference in the shape of the potential peaks between the nonaxial carbon atoms in linkers 1 and 2 (Figure 2b). The nonaxial carbon peaks of linker 2 have well-defined positions in comparison to those of linker 1, indicating that the atoms in linker 2 are more ordered and have much less motion.

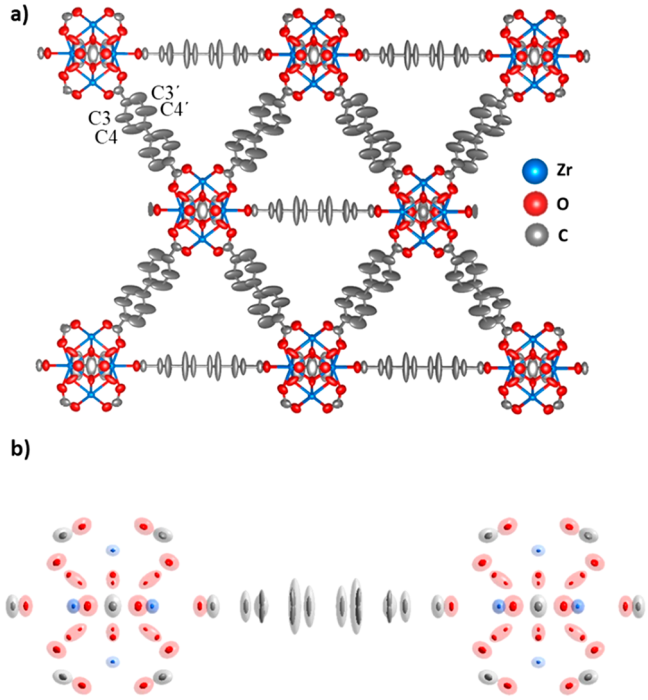

Figure 1. (a) Thermal ellipsoid model (50% probability) of UiO-67 obtained after refinement against cRED data. (b) Superimposed thermal ellipsoid models of UiO-67 obtained from cRED (transparent) and SCXRD (solid) data. Atomic bonds are removed for clarity.

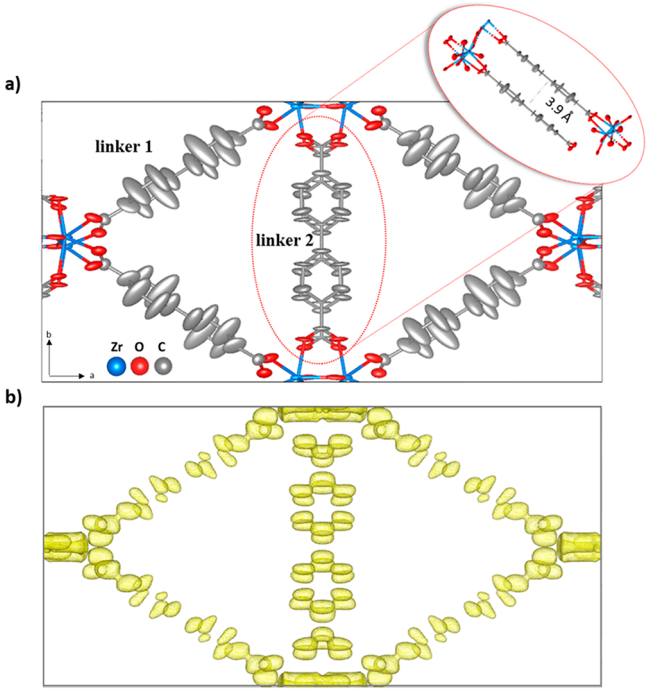

Figure 2. (a) Thermal ellipsoid model (50% probability) of MIL-140C obtained after refinement against cRED data. The model is viewed along the [001] direction. (b) The electrostatic potential map, which was contoured at the 2σ level.

https://doi.org/10.1021/jacs.1c08354
J. Am. Chem. Soc. 2021, 143, 17947−17952

The ellipsoids of linker 1 elongate perpendicularly to their linker planes. Within the MOF structure, linkers 1 and 2 have different chemical environments. For linker 2, the distance between a pair of its linker planes is 3.9 Å. This indicates a weak $\pi-\pi$ interaction, which stabilizes the molecules. As a result, linker 2 molecules are confined in their position, resulting in smaller ellipsoids and more localized potential peaks. In contrast, linker 1 does not form any interaction with other linkers and its large spatial freedom could give raise to molecular motions. Indeed, its stretched ellipsoids resemble the dynamic behavior of the bpdc molecules in UiO-67.

As thermal ellipsoids are an expression of atomic anisotropic displacement parameters (ADPs), we further explore the ADPs obtained by cRED data to better understand the structural details of MIL-140C. We collected data at room temperature (298 K) and cryogenic temperature (98 K), and investigated the behaviors of the ADPs. At each temperature, nine individual data sets were collected from different crystals, which were combined to generate three merged data sets, each from three individual data sets (Tables S3 and S4). We performed anisotropic structure refinement against each of the merged data sets of MIL-140C and plotted the three eigenvalues ($\lambda1$, $\lambda2$, and $\lambda3$) of the four nonaxial carbon atoms of each linker calculated from the corresponding ADPs,[54] as shown in Figure 3c. The eigenvalues describe the mean-square displacements along the three axes of the ellipsoids, with reduced eigenvalues implying smaller atomic displacement.[43] While no significant changes are observed on the eigenvalues at different temperatures, $\lambda1$ values of the nonaxial carbon atoms in both linkers are larger than $\lambda2$ and $\lambda3$ values (Figure 3). While the $\lambda2$ and $\lambda3$ values are similar among all the nonaxial carbon atoms in linkers 1 and 2, the $\lambda1$ values are more than twice as small in linker 2 as those in linker 1. This confirms the rigid behavior of linker 2. It should be noted that many factors, such as incomplete data and dynamic effects, can introduce artifacts on ADPs. However, despite the missing cone due to the preferred crystal orientation of MIL-140C (Figure S6), only the nonaxial carbons in linker 1 exhibit severe elongation of the ellipsoids. This indicates that molecular motion is the predominant factor that causes the elongation. The spatial freedom surrounding linker 1 could facilitate its motion as either small-amplitude librations or π-flips (Figure S7) around the molecular axis.

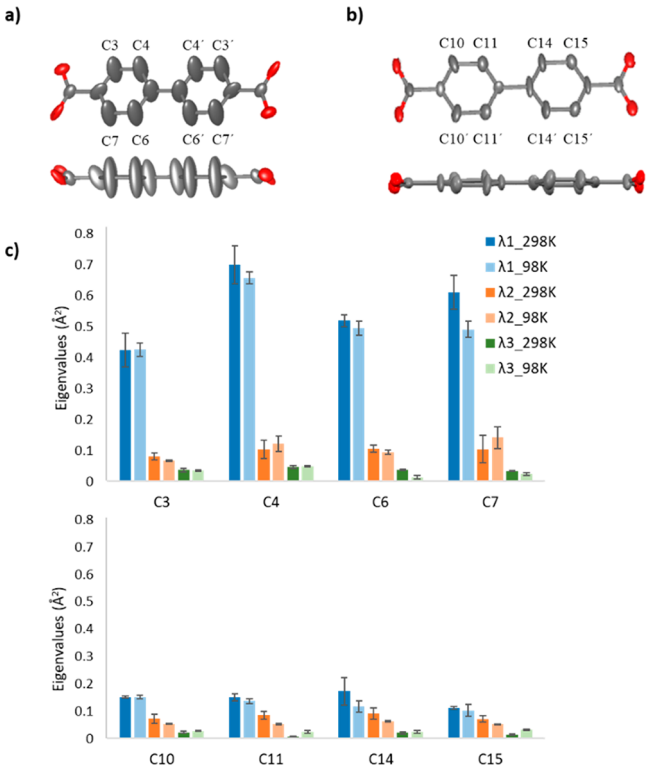

Figure 3. Thermal ellipsoid model (50% probability) of (a) linker 1 and (b) linker 2 in MIL-140C. (c) Eigenvalues ($\lambda1$, $\lambda2$, and $\lambda3$) at 298 and 98 K calculated from the ADPs of the nonaxial carbon atoms in linker 1 (C3, C4, C6, and C7) and linker 2 (C10, C11, C14, and C15).

π-flips are fast high-amplitude motions that occur only when relatively large energy barriers are overcome.[39,55] Solid-state NMR on pure MIL-140C (see the Supporting Information for synthesis details) was applied to further confirm the type of rotational motion of linker 1. The $^{1}H-^{13}C$ CPMAS spectrum at a slow MAS rate of 7 kHz was recorded to allow observation of the ^{13}C chemical shift anisotropy (CSA) pattern (Figure S8). The estimation of the chemical shift anisotropy (δ_{aniso}) as well as the shape of the CSA pattern provides insight into the potential motion of the linkers within the MIL-140C framework. In Figure S8c three pairs of spinning sidebands are observed. The first sideband to the left exhibits substantially higher intensity in comparison to that to the right, whereas the remaining two pairs of sidebands have comparable intensities. This indicates an axially asymmetric NMR shielding tensor and CSA pattern ($\delta_{xx} \neq \delta_{yy} \neq \delta_{zz}$). In the case of rapid linker rotation, the partial averaging of the shielding tensor would occur, and the averaged shielding tensor is expected to display axial symmetry and a narrower CSA pattern.[56,57] For comparison, the low-temperature asymmetric CSA pattern of benzene collapses into an axially symmetric pattern at 223 K due to rapid molecular reorientation,[58] which is not the case for the MIL-140C linkers. Furthermore, we calculated the ^{13}C δ_{aniso} values of the phenyl groups in MIL-140C linkers on the basis of the structural models determined by cRED. The calculated δ_{aniso} values were in the range of 110−190 ppm with a mean δ_{aniso} value of 162 ppm, which is close to our experimental estimate from MIL-140C of ~140 ppm. This together with the axially asymmetric CSA pattern suggests the absence of π-flips in MIL-140C and thus confirms that small-amplitude librational motions generated in the potential well around the central position are the origin of the molecular motions in MIL-140C (Figure 4).

In conclusion, we demonstrate that 3D ED can open new opportunities to reveal molecular motions in MOFs. The structural model and dynamic behavior of UiO-67 obtained from cRED data show a good agreement with those by SCXRD and molecular simulation, confirming that 3D ED can achieve high accuracy in structure determination and can probe molecular motions. Importantly, we also demonstrate that 3D ED can be used to distinguish different extents of molecular motions of the same linker in MIL-140C, where motions are identified in the isolated linkers rather than those reinforced by $\pi-\pi$ interaction. By providing more details on positional specific motions, it could further open the possibility for tailoring different levels of local dynamics in MOFs. Considering the difficulty in obtaining large crystals and pure samples, we envisage 3D ED to be an important technique in studying molecular motions not only in MOFs but also in

https://doi.org/10.1021/jacs.1c08354
J. Am. Chem. Soc. 2021, 143, 17947−17952

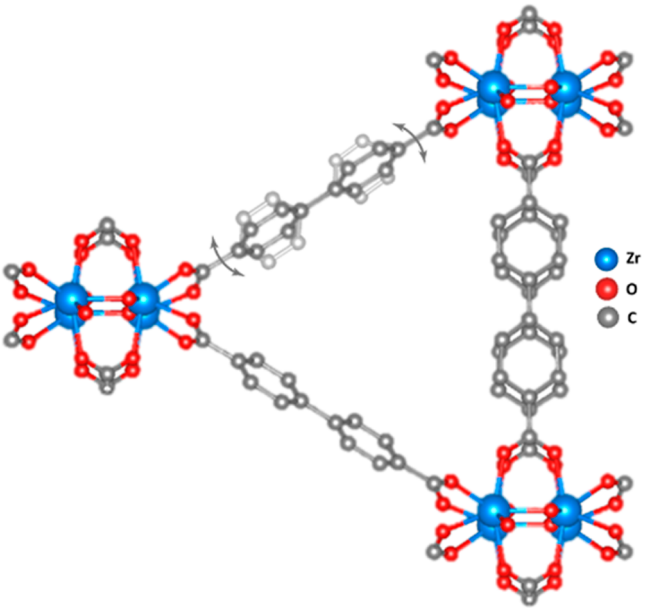

Figure 4. Linker 1 in MIL-140C exhibits small-amplitude librational motions (indicated by the arrows).

other materials, such as covalent organic frameworks and other organic crystals.

■ ASSOCIATED CONTENT

Supporting Information

The Supporting Information is available free of charge at https://pubs.acs.org/doi/10.1021/jacs.1c08354.

Experimental details, SEM, PXRD, structure refinement, and NMR (PDF)

Accession Codes

CCDC 2073254−2073255 and 2087354 contain the supplementary crystallographic data for this paper. These data can be obtained free of charge via www.ccdc.cam.ac.uk/data_request/cif, or by emailing data_request@ccdc.cam.ac.uk, or by contacting The Cambridge Crystallographic Data Centre, 12 Union Road, Cambridge CB2 1EZ, UK; fax: +44 1223 336033.

■ AUTHOR INFORMATION

Corresponding Authors

Xiaodong Zou − *Department of Materials and Environmental Chemistry, Stockholm University, Stockholm SE-106 91, Sweden;* orcid.org/0000-0001-6748-6656; Email: xzou@mmk.su.se

Zhehao Huang − *Department of Materials and Environmental Chemistry, Stockholm University, Stockholm SE-106 91, Sweden;* orcid.org/0000-0002-4575-7870; Email: zhehao.huang@mmk.su.se

Authors

Laura Samperisi − *Department of Materials and Environmental Chemistry, Stockholm University, Stockholm SE-106 91, Sweden*

Aleksander Jaworski − *Department of Materials and Environmental Chemistry, Stockholm University, Stockholm SE-106 91, Sweden;* orcid.org/0000-0002-7156-559X

Gurpreet Kaur − *Department of Organic Chemistry, Stockholm University, Stockholm SE-106 91, Sweden*

Karl Petter Lillerud − *Department of Chemistry, Center for Materials Science and Nanotechnology, University of Oslo, N-0315 Oslo, Norway*

Complete contact information is available at: https://pubs.acs.org/10.1021/jacs.1c08354

Notes

The authors declare no competing financial interest.

■ ACKNOWLEDGMENTS

This work was supported by the Swedish Research Council (VR, 2016-04625, Z.H.; 2017-04321, X.Z.), the Swedish Research Council Formas (2020-00831, Z.H.) and the Knut and Alice Wallenberg Foundation (KAW, 2016.0072). We would like to thank Chris Affolter for the extended help in material synthesis.

■ REFERENCES

(1) Serre, C.; Millange, F.; Thouvenot, C.; Noguès, M.; Marsolier, G.; Louër, D.; Férey, G. Very Large Breathing Effect in the First Nanoporous Chromium(III)-Based Solids: MIL-53 or CrIII(OH)·{O2C−C6H4−CO2}·{HO2C−C6H4−CO2H}x·H2Oy. *J. Am. Chem. Soc.* **2002**, *124* (45), 13519−13526.

(2) Horike, S.; Shimomura, S.; Kitagawa, S. Soft Porous Crystals. *Nat. Chem.* **2009**, *1* (9), 695−704.

(3) Schneemann, A.; Bon, V.; Schwedler, I.; Senkovska, I.; Kaskel, S.; Fischer, R. A. Flexible Metal−Organic Frameworks. *Chem. Soc. Rev.* **2014**, *43* (16), 6062−6096.

(4) Morris, R. E.; Brammer, L. Coordination Change, Lability and Hemilability in Metal−Organic Frameworks. *Chem. Soc. Rev.* **2017**, *46* (17), 5444−5462.

(5) Bennett, T. D.; Cheetham, A. K.; Fuchs, A. H.; Coudert, F.-X. Interplay between Defects, Disorder and Flexibility in Metal-Organic Frameworks. *Nat. Chem.* **2017**, *9* (1), 11−16.

(6) Bigdeli, F.; Lollar, C. T.; Morsali, A.; Zhou, H.-C. Switching in Metal−Organic Frameworks. *Angew. Chem., Int. Ed.* **2020**, *59* (12), 4652−4669.

(7) Kitaura, R.; Seki, K.; Akiyama, G.; Kitagawa, S. Porous Coordination-Polymer Crystals with Gated Channels Specific for Supercritical Gases. *Angew. Chem., Int. Ed.* **2003**, *42* (4), 428−431.

(8) Mohideen, M. I. H.; Xiao, B.; Wheatley, P. S.; McKinlay, A. C.; Li, Y.; Slawin, A. M. Z.; Aldous, D. W.; Cessford, N. F.; Düren, T.; Zhao, X.; Gill, R.; Thomas, K. M.; Griffin, J. M.; Ashbrook, S. E.; Morris, R. E. Protecting Group and Switchable Pore-Discriminating Adsorption Properties of a Hydrophilic−Hydrophobic Metal−Organic Framework. *Nat. Chem.* **2011**, *3* (4), 304−310.

(9) Mason, J. A.; Oktawiec, J.; Taylor, M. K.; Hudson, M. R.; Rodriguez, J.; Bachman, J. E.; Gonzalez, M. I.; Cervellino, A.; Guagliardi, A.; Brown, C. M.; Llewellyn, P. L.; Masciocchi, N.; Long, J. R. Methane Storage in Flexible Metal−Organic Frameworks with Intrinsic Thermal Management. *Nature* **2015**, *527* (7578), 357−361.

(10) Su, J.; Yuan, S.; Wang, H.-Y.; Huang, L.; Ge, J.-Y.; Joseph, E.; Qin, J.; Cagin, T.; Zuo, J.-L.; Zhou, H.-C. Redox-Switchable Breathing Behavior in Tetrathiafulvalene-Based Metal−Organic Frameworks. *Nat. Commun.* **2017**, *8* (1), 1−8.

(11) Das, R. K.; Aijaz, A.; Sharma, M. K.; Lama, P.; Bharadwaj, P. K. Direct Crystallographic Observation of Catalytic Reactions inside the Pores of a Flexible Coordination Polymer. *Chem. - Eur. J.* **2012**, *18* (22), 6866−6872.

(12) Yuan, S.; Zou, L.; Li, H.; Chen, Y.-P.; Qin, J.; Zhang, Q.; Lu, W.; Hall, M. B.; Zhou, H.-C. Flexible Zirconium Metal-Organic Frameworks as Bioinspired Switchable Catalysts. *Angew. Chem., Int. Ed.* **2016**, *55* (36), 10776−10780.

(13) Lo, S.-H.; Feng, L.; Tan, K.; Huang, Z.; Yuan, S.; Wang, K.-Y.; Li, B.-H.; Liu, W.-L.; Day, G. S.; Tao, S.; Yang, C.-C.; Luo, T.-T.; Lin, C.-H.; Wang, S.-L.; Billinge, S. J. L.; Lu, K.-L.; Chabal, Y. J.; Zou, X.; Zhou, H.-C. Rapid Desolvation-Triggered Domino Lattice Rearrange-

ment in a Metal−Organic Framework. *Nat. Chem.* **2020**, *12* (1), 90−97.
(14) Gu, C.; Hosono, N.; Zheng, J.-J.; Sato, Y.; Kusaka, S.; Sakaki, S.; Kitagawa, S. Design and Control of Gas Diffusion Process in a Nanoporous Soft Crystal. *Science* **2019**, *363* (6425), 387−391.
(15) Lin, R.-B.; Li, L.; Wu, H.; Arman, H.; Li, B.; Lin, R.-G.; Zhou, W.; Chen, B. Optimized Separation of Acetylene from Carbon Dioxide and Ethylene in a Microporous Material. *J. Am. Chem. Soc.* **2017**, *139* (23), 8022−8028.
(16) Carrington, E. J.; McAnally, C. A.; Fletcher, A. J.; Thompson, S. P.; Warren, M.; Brammer, L. Solvent-Switchable Continuous-Breathing Behaviour in a Diamondoid Metal−Organic Framework and Its Influence on CO 2 versus CH 4 Selectivity. *Nat. Chem.* **2017**, *9* (9), 882−889.
(17) Dong, Q.; Zhang, X.; Liu, S.; Lin, R.-B.; Guo, Y.; Ma, Y.; Yonezu, A.; Krishna, R.; Liu, G.; Duan, J.; Matsuda, R.; Jin, W.; Chen, B. Tuning Gate-Opening of a Flexible Metal−Organic Framework for Ternary Gas Sieving Separation. *Angew. Chem., Int. Ed.* **2020**, *59* (50), 22756−22762.
(18) Fairen-Jimenez, D.; Moggach, S. A.; Wharmby, M. T.; Wright, P. A.; Parsons, S.; Düren, T. Opening the Gate: Framework Flexibility in ZIF-8 Explored by Experiments and Simulations. *J. Am. Chem. Soc.* **2011**, *133* (23), 8900−8902.
(19) Murdock, C. R.; McNutt, N. W.; Keffer, D. J.; Jenkins, D. M. Rotating Phenyl Rings as a Guest-Dependent Switch in Two-Dimensional Metal−Organic Frameworks. *J. Am. Chem. Soc.* **2014**, *136* (2), 671−678.
(20) Katsoulidis, A. P.; Antypov, D.; Whitehead, G. F. S.; Carrington, E. J.; Adams, D. J.; Berry, N. G.; Darling, G. R.; Dyer, M. S.; Rosseinsky, M. J. Chemical Control of Structure and Guest Uptake by a Conformationally Mobile Porous Material. *Nature* **2019**, *565* (7738), 213−217.
(21) Trenholme, W. J. F.; Kolokolov, D. I.; Bound, M.; Argent, S. P.; Gould, J. A.; Li, J.; Barnett, S. A.; Blake, A. J.; Stepanov, A. G.; Besley, E.; Easun, T. L.; Yang, S.; Schröder, M. Selective Gas Uptake and Rotational Dynamics in a (3,24)-Connected Metal−Organic Framework Material. *J. Am. Chem. Soc.* **2021**, *143* (9), 3348−3358.
(22) He, T.; Huang, Z.; Yuan, S.; Lv, X.-L.; Kong, X.-J.; Zou, X.; Zhou, H.-C.; Li, J.-R. Kinetically Controlled Reticular Assembly of a Chemically Stable Mesoporous Ni(II)-Pyrazolate Metal−Organic Framework. *J. Am. Chem. Soc.* **2020**, *142* (31), 13491−13499.
(23) Carraro, F.; Velásquez-Hernández, M. de J.; Astria, E.; Liang, W.; Twight, L.; Parise, C.; Ge, M.; Huang, Z.; Ricco, R.; Zou, X.; Villanova, L.; Kappe, C. O.; Doonan, C.; Falcaro, P. Phase Dependent Encapsulation and Release Profile of ZIF-Based Biocomposites. *Chem. Sci.* **2020**, *11* (13), 3397−3404.
(24) Liu, L.; Zhang, D.; Zhu, Y.; Han, Y. Bulk and Local Structures of Metal−Organic Frameworks Unravelled by High-Resolution Electron Microscopy. *Commun. Chem.* **2020**, *3* (1), 1−14.
(25) Gong, X.; Gnanasekaran, K.; Chen, Z.; Robison, L.; Wasson, M. C.; Bentz, K. C.; Cohen, S. M.; Farha, O. K.; Gianneschi, N. C. Insights into the Structure and Dynamics of Metal−Organic Frameworks via Transmission Electron Microscopy. *J. Am. Chem. Soc.* **2020**, *142* (41), 17224−17235.
(26) Portolés-Gil, N.; Lanza, A.; Aliaga-Alcalde, N.; Ayllón, J. A.; Gemmi, M.; Mugnaioli, E.; López-Periago, A. M.; Domingo, C. Crystalline Curcumin BioMOF Obtained by Precipitation in Supercritical CO2 and Structural Determination by Electron Diffraction Tomography. *ACS Sustainable Chem. Eng.* **2018**, *6* (9), 12309−12319.
(27) Yuan, S.; Qin, J.-S.; Xu, H.-Q.; Su, J.; Rossi, D.; Chen, Y.; Zhang, L.; Lollar, C.; Wang, Q.; Jiang, H.-L.; Son, D. H.; Xu, H.; Huang, Z.; Zou, X.; Zhou, H.-C. [Ti8Zr2O12(COO)16] Cluster: An Ideal Inorganic Building Unit for Photoactive Metal−Organic Frameworks. *ACS Cent. Sci.* **2018**, *4* (1), 105−111.
(28) Leubner, S.; Zhao, H.; Van Velthoven, N.; Henrion, M.; Reinsch, H.; De Vos, D. E.; Kolb, U.; Stock, N. Expanding the Variety of Zirconium-based Inorganic Building Units for Metal−Organic Frameworks. *Angew. Chem.* **2019**, *131* (32), 11111−11116.
(29) Smolders, S.; Willhammar, T.; Krajnc, A.; Sentosun, K.; Wharmby, M. T.; Lomachenko, K. A.; Bals, S.; Mali, G.; Roeffaers, M. B. J.; De Vos, D. E.; Bueken, B. A Titanium(IV)-Based Metal−Organic Framework Featuring Defect-Rich Ti-O Sheets as an Oxidative Desulfurization Catalyst. *Angew. Chem.* **2019**, *131* (27), 9258−9263.
(30) Grape, E. S.; Flores, J. G.; Hidalgo, T.; Martínez-Ahumada, E.; Gutiérrez-Alejandre, A.; Hautier, A.; Williams, D. R.; O'Keeffe, M.; Öhrström, L.; Willhammar, T.; Horcajada, P.; Ibarra, I. A.; Inge, A. K. A Robust and Biocompatible Bismuth Ellagate MOF Synthesized Under Green Ambient Conditions. *J. Am. Chem. Soc.* **2020**, *142* (39), 16795−16804.
(31) Cichocka, M. O.; Liang, Z.; Feng, D.; Back, S.; Siahrostami, S.; Wang, X.; Samperisi, L.; Sun, Y.; Xu, H.; Hedin, N.; Zheng, H.; Zou, X.; Zhou, H.-C.; Huang, Z. A Porphyrinic Zirconium Metal−Organic Framework for Oxygen Reduction Reaction: Tailoring the Spacing between Active-Sites through Chain-Based Inorganic Building Units. *J. Am. Chem. Soc.* **2020**, *142* (36), 15386−15395.
(32) Dou, J. H.; Arguilla, M. Q.; Luo, Y.; Li, J.; Zhang, W.; Sun, L.; Mancuso, J. L.; Yang, L.; Chen, T.; Parent, L. R.; Skorupskii, G.; Libretto, N. J.; Sun, C.; Yang, M. C.; Dip, P. V.; Brignole, E. J.; Miller, J. T.; Kong, J.; Hendon, C. H.; Sun, J.; Dinc, ăM. Atomically Precise Single-Crystal Structures of Electrically Conducting 2D Metal−Organic Frameworks. *Nat. Mater.* **2021**, *20*, 222−228.
(33) Ge, M.; Wang, Y.; Carraro, F.; Liang, W.; Roostaeinia, M.; Siahrostami, S.; Proserpio, D. M.; Doonan, C.; Falcaro, P.; Zheng, H.; Zou, X.; Huang, Z. High-Throughput Electron Diffraction Reveals a Hidden Novel Metal−Organic Framework for Electrocatalysis. *Angew. Chem., Int. Ed.* **2021**, *60* (20), 11391−11397.
(34) Hynek, J.; Brázda, P.; Rohlícek, J.; Londesborough, M. G. S.; Demel, J. Phosphinic Acid Based Linkers: Building Blocks in Metal−Organic Framework Chemistry. *Angew. Chem., Int. Ed.* **2018**, *57* (18), 5016−5019.
(35) Kolb, U.; Gorelik, T.; Kübel, C.; Otten, M. T.; Hubert, D. Towards Automated Diffraction Tomography: Part I—Data Acquisition. *Ultramicroscopy* **2007**, *107* (6), 507−513.
(36) Zhang, D.; Oleynikov, P.; Hovmöller, S.; Zou, X. Collecting 3D Electron Diffraction Data by the Rotation Method. *Z. Kristallogr.* **2010**, *225*, 94−102.
(37) Gemmi, M.; Mugnaioli, E.; Gorelik, T. E.; Kolb, U.; Palatinus, L.; Boullay, P.; Hovmöller, S.; Abrahams, J. P. 3D Electron Diffraction: The Nanocrystallography Revolution. *ACS Cent. Sci.* **2019**, *5* (8), 1315−1329.
(38) Huang, Z.; Willhammar, T.; Zou, X. Three-Dimensional Electron Diffraction for Porous Crystalline Materials: Structural Determination and Beyond. *Chem. Sci.* **2021**, *12* (4), 1206−1219.
(39) Kolokolov, D. I.; Stepanov, A. G.; Guillerm, V.; Serre, C.; Frick, B.; Jobic, H. Probing the Dynamics of the Porous Zr Terephthalate UiO-66 Framework Using 2H NMR and Neutron Scattering. *J. Phys. Chem. C* **2012**, *116* (22), 12131−12136.
(40) Shustova, N. B.; Ong, T.-C.; Cozzolino, A. F.; Michaelis, V. K.; Griffin, R. G.; Dincă, M. Phenyl Ring Dynamics in a Tetraphenylethylene-Bridged Metal−Organic Framework: Implications for the Mechanism of Aggregation-Induced Emission. *J. Am. Chem. Soc.* **2012**, *134* (36), 15061−15070.
(41) Ryder, M. R.; Civalleri, B.; Bennett, T. D.; Henke, S.; Rudić, S.; Cinque, G.; Fernandez-Alonso, F.; Tan, J.-C. Identifying the Role of Terahertz Vibrations in Metal-Organic Frameworks: From Gate-Opening Phenomenon to Shear-Driven Structural Destabilization. *Phys. Rev. Lett.* **2014**, *113* (21), 215502.
(42) Peterson, V. K.; Kearley, G. J.; Wu, Y.; Ramirez-Cuesta, A. J.; Kemner, E.; Kepert, C. J. Local Vibrational Mechanism for Negative Thermal Expansion: A Combined Neutron Scattering and First-Principles Study. *Angew. Chem., Int. Ed.* **2010**, *49* (3), 585−588.
(43) Smeets, S.; Parois, P.; Bürgi, H.-B.; Lutz, M. Temperature-Dependent Analysis of Thermal Motion, Disorder and Structures of Tris(Ethylenediamine)Zinc(II) Sulfate and Tris(Ethylenediamine)-Copper(II) Sulfate. *Acta Crystallogr., Sect. B: Struct. Sci.* **2011**, *67* (1), 53−62.

https://doi.org/10.1021/jacs.1c08354
J. Am. Chem. Soc. 2021, 143, 17947−17952

(44) Catalano, L.; Pérez-Estrada, S.; Terraneo, G.; Pilati, T.; Resnati, G.; Metrangolo, P.; Garcia-Garibay, M. A. Dynamic Characterization of Crystalline Supramolecular Rotors Assembled through Halogen Bonding. *J. Am. Chem. Soc.* **2015**, *137* (49), 15386−15389.
(45) Navarro-Huerta, A.; Jellen, M. J.; Arcudia, J.; Teat, S. J.; Toscano, R. A.; Merino, G.; Rodríguez-Molina, B. Tailoring the Cavities of Hydrogen-Bonded Amphidynamic Crystals Using Weak Contacts: towards faster molecular machines. *Chem. Sci.* **2021**, *12*, 2181−2188.
(46) Cichocka, M. O.; Ångström, J.; Wang, B.; Zou, X.; Smeets, S. High-throughput continuous rotation electron diffraction data acquisition via software automation. *J. Appl. Crystallogr.* **2018**, *51*, 1652−1661.
(47) Kaur, G.; Øien-Ødegaard, S.; Lazzarini, A.; Chavan, S. M.; Bordiga, S.; Lillerud, K. P.; Olsbye, U. Controlling the Synthesis of Metal−Organic Framework UiO-67 by Tuning Its Kinetic Driving Force. *Cryst. Growth Des.* **2019**, *19* (8), 4246−4251.
(48) Yun, Y.; Wan, W.; Rabbani, F.; Su, J.; Hovmöller, S.; Johnsson, M.; Zou, X. Phase identification and structure determination from multiphasic crystalline powder samples by rota-tion electron diffraction. *J. Appl. Crystallogr.* **2014**, *47*, 2048−2054.
(49) Cavka, J. H.; Jakobsen, S.; Olsbye, U.; Guillou, N.; Lamberti, C.; Bordiga, S.; Lillerud, K. P. A New Zirconium Inorganic Building Brick Forming Metal Organic Frameworks with Exceptional Stability. *J. Am. Chem. Soc.* **2008**, *130* (42), 13850−13851.
(50) Guillerm, V.; Ragon, F.; Dan-Hardi, M.; Devic, T.; Vishnuvarthan, M.; Campo, B.; Vimont, A.; Clet, G.; Yang, Q.; Maurin, G.; Férey, G.; Vittadini, A.; Gross, S.; Serre, C. A Series of Isoreticular, Highly Stable, Porous Zirconium Oxide Based Metal−Organic Frameworks. *Angew. Chem., Int. Ed.* **2012**, *51* (37), 9267−9271.
(51) Øien, S.; Wragg, D.; Reinsch, H.; Svelle, S.; Bordiga, S.; Lamberti, C.; Lillerud, K. P. Detailed Structure Analysis of Atomic Positions and Defects in Zirconium Metal−Organic Frameworks. *Cryst. Growth Des.* **2014**, *14* (11), 5370−5372.
(52) Hummel, W.; Raselli, A.; Bürgi, H.-B. Analysis of Atomic Displacement Parameters and Molecular Motion in Crystals. *Acta Crystallogr., Sect. B: Struct. Sci.* **1990**, *46* (5), 683−692.
(53) Hobday, C. L.; Marshall, R. J.; Murphie, C. F.; Sotelo, J.; Richards, T.; Allan, D. R.; Düren, T.; Coudert, F.-X.; Forgan, R. S.; Morrison, C. A.; Moggach, S. A.; Bennett, T. D. A Computational and Experimental Approach Linking Disorder, High-Pressure Behavior, and Mechanical Properties in UiO Frameworks. *Angew. Chem., Int. Ed.* **2016**, *55* (7), 2401−2405.
(54) Grosse- Kunstleve, R. W.; Adams, P. D. On the handling of atomic anisotropic displacement parameters. *J. Appl. Crystallogr.* **2002**, *35*, 477−480.
(55) Kolokolov, D. I.; Stepanov, A. G.; Guillerm, V.; Deivic, T.; Serre, C.; Férey, G. B.; Jobic, H. Dynamics of Benzene Rings in MIL-53(Cr) and MIL-47(V) Frameworks Studied by ^{2}H NMR Spectroscopy. *Angew. Chem., Int. Ed.* **2010**, *49* (28), 4791−4794.
(56) Gall, C. M.; Cross, T. A.; DiVerdi, J. A.; Opella, S. J. Protein Dynamics by Solid-State NMR: Aromatic Rings of the Coat Protein in Fd Bacteriophage. *Proc. Natl. Acad. Sci. U. S. A.* **1982**, *79* (1), 101−105.
(57) Duncan, T. M. 13C Chemical Shieldings in Solids. *J. Phys. Chem. Ref. Data* **1987**, *16* (1), 125−151.
(58) Pines, A.; Gibby, M. G.; Waugh, J. S. Proton-Enhanced Nuclear Induction Spectroscopy 13C Chemical Shielding Anisotropy in Some Organic Solids. *Chem. Phys. Lett.* **1972**, *15* (3), 373−376.

https://doi.org/10.1021/jacs.1c08354
J. Am. Chem. Soc. 2021, 143, 17947−17952